19th INTERNATIONAL CONGRESS ON ACOUSTICS
MADRID, 2-7 SEPTEMBER 2007

OPTIMAL SPACE-TIME FINITE DIFFERENCE SCHEMES FOR EXPERIMENTAL BOOTH DESIGN

PACS: 43.55.Ka

Naka, Yusuke[1]; Oberai, Assad A.[2]; Shinn-Cunningham, Barbara G.[3]
[1]Japan Aerospace Exploration Agency; 6-13-1 Osawa, Mitaka, Tokyo 181-0015, Japan; ynaka@chofu.jaxa.jp
[2]Rensselaer Polytechnic Institute; 5048 JEC, 8th St., Troy, NY 12180, U.S.A.; oberaa@rpi.edu
[3]Boston University; 677 Beacon St., Boston, MA 02215, U.S.A.; shinn@cns.bu.edu

ABSTRACT
In numerical simulations of acoustic phenomena in cavities and indoor spaces, where reflections and reverberation make it necessary to calculate the solution for a long duration, it is essential to reduce dispersion and dissipation errors, which accumulate over time. The authors have developed a new, efficient, high-order finite difference scheme that is suitable for this application. In this scheme, which is referred to as the optimal space-time (OST) scheme, the total error resulting from the discretization in space and time is minimized. The solution is very accurate (8.6 % error after 1 second for a maximum frequency of 5,000 Hz) with relatively coarse spatial (6 grid points per wavelength) and temporal (CFL = 1.0) resolution. In this study, the OST scheme is applied for designing a booth to be used in subjective psychoacoustic experiments. The effects of wall absorption and listener position are investigated. The results indicate that these factors are especially influential at high frequencies. Results suggest that in order to ensure that a listener receives the intended sound, special care must be taken when presenting stimuli with high-frequency content through a loudspeaker in a booth.

INTRODUCTION
With the rapid growth of computers, numerical simulations of acoustics based on the wave theory, which are more accurate but require more computations than traditional approaches based on the ray acoustics, have been applied recently to various indoor spaces. Several numerical methods, such as the boundary element method, the finite element method, and the finite-difference time-domain method, have been used for solving the wave equation either in the time or frequency domain. These applications have been limited to acoustically small domains (i.e., for small spaces or low-frequency range) because conventional numerical methods incur dispersion (phase) and dissipation (amplitude) errors that accumulate and grow with increasing problem size. Therefore, more accurate and more efficient numerical methods are required for acoustically large cavities and indoor spaces. With this in mind, the authors have developed a new, high-order finite difference scheme with minimal dispersion and dissipation errors, referred to as the optimal space-time (OST) scheme [1, 2], for solving the scalar wave equation in the time domain. In this study, the OST finite difference scheme is used for evaluating the sound stimuli presented to subjects in booths like those used in psychoacoustic experiments. The effects of two important factors, namely wall absorption and listener positions, are investigated.

OPTIMAL SPACE-TIME (OST) FINITE DIFFERENCE SCHEMES
In this section, the optimal space-time (OST) finite difference scheme is briefly reviewed. For the details of this scheme, the reader is referred to [1, 2].

In the time domain, the wave equation must be discretized in time in addition to space. Both types of discretization (in space and time) create dispersion (phase) and dissipation (magnitude) errors. Although several techniques have been developed to reduce these errors, most of such techniques have considered the errors in time and space separately [3, 4].

However, since the total accuracy of a numerical method is affected by the combination of the spatial and temporal discretization, in the OST scheme, the total error is minimized.

We consider the following second-order scalar wave equation in the time domain:

$$\ddot{p}(\mathbf{x},t) - c^2 \nabla^2 p(\mathbf{x},t) = 0 , \quad \text{(Eq. 1)}$$

where p is the acoustic pressure, $\mathbf{x}$ the position vector, t the time, c the speed of sound, and a dot indicates the partial derivative with respect to time. Discretization of (Eq. 1) in both space and time leads to the following linear system:

$$\mathbf{y}(t_{n+1}) = \mathbf{B}\mathbf{y}(t_n) . \quad \text{(Eq. 2)}$$

In (Eq. 2),

$$\mathbf{y}(t_n) = \begin{bmatrix} \dot{\mathbf{p}}(t_n) \\ \mathbf{p}(t_n) \end{bmatrix}, \quad \text{(Eq. 3)}$$

where $\mathbf{p}$ is a vector of acoustic pressure at spatially discretized grid points, and $t_n = n\Delta t$ is the n-th time step. $\mathbf{B}$ is a matrix consisting of spatial and temporal discretization coefficients. In OST schemes, these coefficients are determined so as to minimize the total dispersion and dissipation error for solutions propagating in all directions and for all frequencies up to a predetermined criterion, while keeping the time-integration scheme stable. It is also possible to prescribe a certain formal (Taylor-series) order of accuracy in optimizing the spatial and temporal discretization schemes.

The accuracy of an OST scheme depends on several parameters, such as the number of spatial grid points per wave length and the Courant-Friedrichs-Lewy (CFL) number. Therefore, desirable or necessary accuracy might be obtained by carefully determining these parameters. For example, in three dimensions, 1.7 % error can be attained after propagating the solution for 1,000 wavelengths with a resolution of just 6 spatial points per wavelength and a CFL number of unity when the 25-point, second-order spatial stencil (9 points in each direction) is combined with the 10-stage, sixth-order time integration scheme. The error of the conventional Taylor-series based finite difference scheme with the same computational cost is 112.4 %.

NUMRICAL SIMULATIONS

The OST finite difference scheme is applied to solve the wave equation (Eq.1) with the frequency-independent impedance boundary conditions given by

$$p_{,n}(\mathbf{x}_{\mathrm{bdry}}) = \frac{\rho}{Z} \dot{p}(\mathbf{x}_{\mathrm{bdry}}), \quad \text{(Eq. 4)}$$

and with the initial conditions given by

$$p(\mathbf{x},0) = \begin{cases} \cos^2\left(\dfrac{\pi(x-x_s)}{w_s}\right)\cos^2\left(\dfrac{\pi(y-y_s)}{w_s}\right)\cos^2\left(\dfrac{\pi(z-z_s)}{w_s}\right), & \text{if } |x-x_s| \le w_s, |y-y_s| \le w_s, |z-z_s| \le w_s \\ 0, & \text{otherwise} \end{cases} \quad \text{(Eq. 5)}$$

$$\dot{p}(\mathbf{x},0) = 0 . \quad \text{(Eq. 6)}$$

In (Eq. 4) – (Eq. 6), $p_{,n}$ is the outward normal derivative of p at $\mathbf{x}_{\mathrm{bdry}}$ on a boundary, ρ the density of air, Z the impedance on a boundary, (x_s, y_s, z_s) the center position of the sound source, and w_s the half width of the source.

In this study, we consider a cubic booth with the dimension of 2.4 m in each direction. Although relatively small, this booth is large enough for one subject, and booths of similar and smaller sizes are widely used. One class of examples are the sonic boom simulators [5].

A simple listener model shown in Fig. 1 is placed in the computational domain, and the responses at the left and right ear positions are recorded. The speed of sound and the air density are set at c = 340 m/s and ρ = 1.0 kg/m^3, respectively. The impedance Z is given as a real number corresponding to a predetermined absorption coefficient. The booth is spatially discretized by 256 grid points in each direction, resulting in the grid size h = 9.41×10^{-3} m. The

CFL number, defined by CFL = $c\Delta t / h$, is set at 1.0, which corresponds to the time step Δt = 2.77×10^{-5} seconds for the given grid size. The half width of the source is set at w_s = 6 h = 5.65×10^{-2} m. This sound source has the peak frequency at around 3 kHz. The OST scheme with the 25-point, second-order spatial stencil and the 10-stage, sixth-order time-integration scheme that is accurate up to 6 grid points per wavelength is used. Hence, the highest resolved frequency is about 6 kHz. The OST finite difference code is implemented on the IBM Blue Gene platform at Boston University. For the above-mentioned conditions, it takes about 3 hours to compute 20,000 time steps (0.55 seconds of response) on 512 computer nodes.

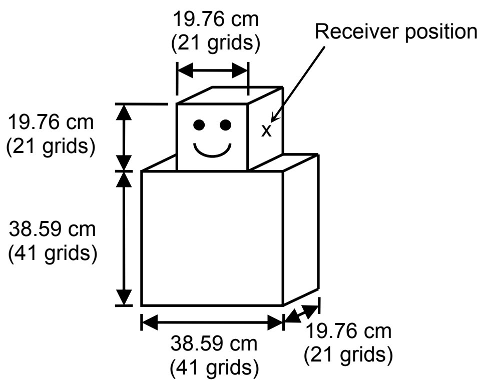

Figure 1.- Simple listener model

NUMRICAL RESULTS 1: WALL ABSORPTION

Absorption on the boundaries is one of the most important acoustic factors in enclosed, reverberant spaces. In order to investigate the effects of the wall absorption, the OST finite difference scheme was implemented for different values of absorption coefficients α on the walls, namely α = 0.1, 0.3, 0.5, 0.7, 0.9. The absorption coefficients on the other surfaces were fixed: 0.5 on the floor and ceiling and 0.1 on the surfaces of the listener model. The position of the listener (the center of the head) was fixed at the center of the booth (at position (1.2, 1.2, 1.2)), while the source was 1 m in front of the listener at position (1.2, 2.2, 1.2).

Figure 2 shows the first 0.1 seconds of the calculated responses at the listener's ear as a function of time for different absorption conditions. Since the responses at the left and right ears are identical due to symmetry, only one response is shown for each value of absorption coefficient. In Fig. 2, the effects of absorption can be clearly observed. The signal decays faster for larger absorption. In addition, distinct packets of acoustic energy are observed with increasing absorption. As absorption on the side walls increases, reflections from these surfaces become weaker. As a result, the pulses traveling back and forth between the ceiling and floor, which reach the receiver at nearly constant time intervals, becomes more dominant, making it easier to see each discrete response in time.

Figure 3 shows the 1/3-octave band frequency spectra of 0.45 seconds (16,384 time steps) of the responses shown in Fig. 2. The sound pressure level is higher for larger wall absorption as expected, except in a small frequency band around 100 Hz. This is probably related to the acoustic mode of the booth. If all boundaries are rigid, the frequencies for the first three modes for the booth are 70.8, 100.2, 122.7 Hz. For all these modes, the center of the booth (which is also the listener location in this case) is a node with zero acoustic pressure. Therefore, close to these frequencies, the acoustic energy in the neighborhood of the listener is small when the absorption coefficient is small. As the wall absorption increases, the mode shapes change and the location of the node may move away from the center of the booth.

The lowest mode that has an anti-node at the center of the booth has a frequency of 141.7 Hz. We observe that above this frequency, larger absorption results in less energy. In addition to larger energy loss at reflections, changes in mode shapes may also contribute to the greater absorption at high frequencies: the locations of the anti-nodes may be farther from the center of the booth at higher absorption levels. However, in addition, the spectral shape of the response differs in the high-frequency range for the different absorption levels. These patterns are likely to depend on the exact three-dimensional locations of the anti-nodes in the booth, as well as the reflections from and refraction around the listener. Although we do not discuss the perceptive effects of these spectra here because it is beyond the scope of this paper, such research would be of interest from a psychoacoustic point of view and would be important for designing psychoacoustic experiments.

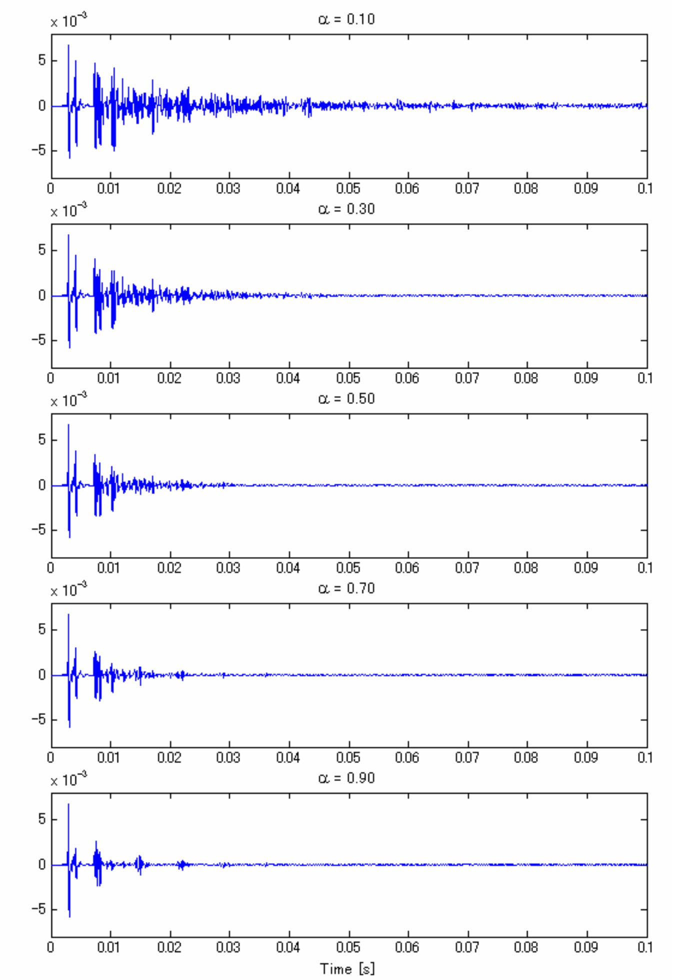

Figure 2.- Responses at the listener's ear for different wall absorption

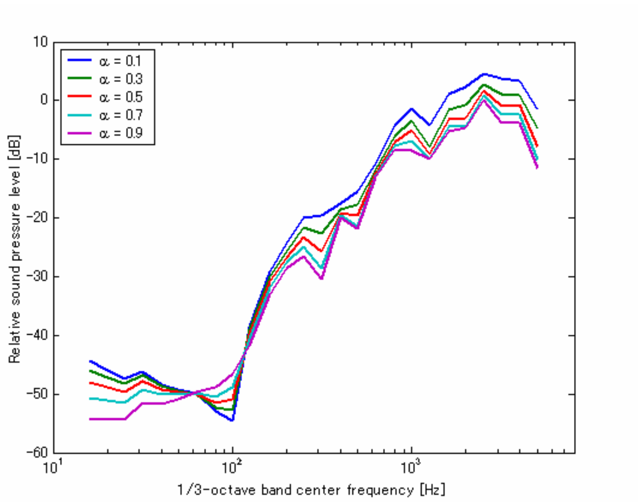

Figure 3.-Frequency spectra for different wall absorption

NUMRICAL RESULTS 2: LISTENER POSITIONS

In many cases, the position of a subject is expected to be fixed during a psychoacoustic experiment. The listener, however, may slightly move his/her head. Also, the ear positions are different from a subject to another. In order to investigate the effects of such small changes in listener position, which are difficult to examine by measurements, the response at the listener's ears was calculated by the OST finite difference scheme for different listener positions.

The listener model was placed either at the center of the booth, 4.7 cm or 9.4 cm left from the center. The corresponding coordinates of the center of the head are (1.2, 1.2, 1.2), (1.153, 1.2, 1.2), and (1.106, 1.2, 1.2), respectively. The source position was fixed in space at (1.2, 2.2, 1.2). The absorption coefficients were fixed at 0.5 on all booth boundaries and 0.1 on the surfaces of the listener model.

Figure 4 shows the first 0.1 seconds of the responses at the listener's left and right ears. In this figure, it is observed that when the listener is 9.4 cm left from the exact center of the booth, the "wave packets" are more distinct (narrower) and their magnitudes are larger, especially at the right ear. This can be explained by considering the position of the ear. When the center of the head is 9.4 cm left from the center of the booth, the right ear of the listener is located very near (only 0.48 cm apart from) the booth center. Therefore, the reflected pulses from the walls, ceiling, and floor arrive at this point almost at the same time, due to symmetry and the source location (at the center in the x- and z-directions).

Figure 5 shows the 1/3-octave band spectra obtained from the first 0.45 seconds (16,384 time steps) of the responses shown in Fig. 4. The rank order of the spectral levels is maintained at all frequencies up to 1 kHz. Again, the ordering can be explained by considering the ear position. The nearer to the center, the larger is the spectrum. Beyond 1 kHz, no specific trend is observed in the change of the spectra with listener position. There are variations, however, which appear uncorrelated. We believe that this is because the wavelength in this regime (e.g., 11.3 cm at 3 kHz) is comparable to both the size of the listener model (19.8 cm) and to the variation in the listener location (9.4 cm).

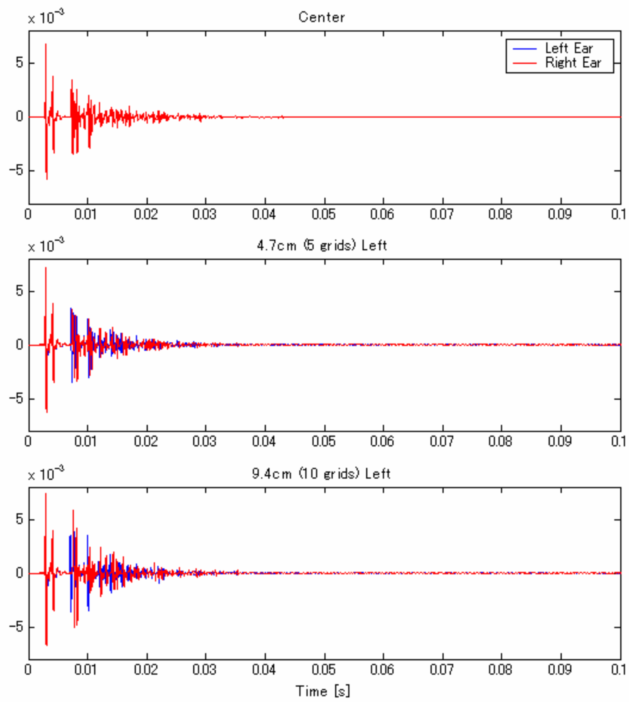

Figure 4.-Responses at the listener's ears for different listener positions

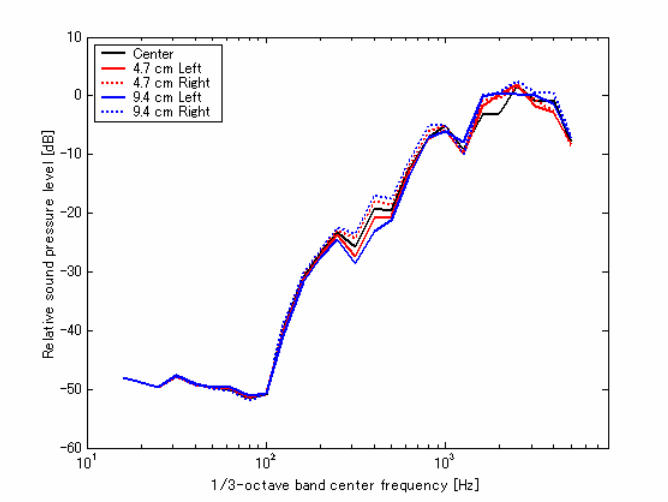

Figure 5.-Frequency spectra for different listener positions

While most of the changes in sound pressure at the listener's ear are relatively small, they are nonetheless large enough to be detectable. The just-noticeable difference in intensity is on the order of 1-2 dB across the range of audible frequencies. The current results show that small listener movements can cause changes in the received sound intensity at the ears that exceed these thresholds in the high-frequency, audible range.

CONCLUSIONS

The optimal space-time (OST) finite difference scheme was applied in designing a booth like is often used for psychoacoustic experiments. The effects of the wall absorption and changes in listener position were investigated. Numerical results indicate that these factors strongly affect the sound received at the listeners' ears, especially in the high-frequency range. It is also concluded that the effect of these factors on the sound spectra is complicated and difficult to predict without detailed analysis of the wave propagation phenomenon. Although the practical impact of these variations in the spectrum on sound perception is not investigated and are left for future research, it is suggested that wall materials and listener position should be carefully determined if sound stimuli containing high-frequency components are to be used. Careful design of synthetic sound stimuli accounting for these features is also suggested in order to present the intended sound at the listener's ears.

ACKNOWLEDGEMENTS

The authors are grateful to Boston University for use of the IBM Blue Gene platform.

References: [1] Y. Naka: Numerical methods for solving the large-scale wave equation with the application to room acoustics. Ph.D. Dissertation, Boston University (2006).

[2] Y. Naka, A. A. Oberai, B. G. Shinn-Cunningham: Optimal space-time finite difference schemes for the second-order scalar wave equation. Submitted to Computer Methods in Applied Mechanics and Engineering.

[3] C. K. W. Tam, J. C. Webb: Dispersion-relation-preserving finite difference schemes for computational acoustics. Journal of Computational Physics **107** (1993) 262-281.

[4] F. Q. Hu, M. Y. Hussaini, J. L. Manthey: Low-dissipation and low-dispersion Runge-Kutta schemes for computational acoustics. Journal of Computational Physics **124** (1996) 177-191.

[5] J. D. Leatherwood, K. P. Shepherd, B. M. Sullivan: A new simulator for assessing subjective effects of sonic booms. NASA Technical Memorandum 104150 (1991).